

High- Q oscillator torque magnetometer

R. D. Biggar and J. M. Parpia

The Materials Science Center and Laboratory of Atomic & Solid State Physics, Cornell University, Ithaca, New York 14853

(Received 28 April 1998; accepted for publication 27 July 1998)

We describe a torque magnetometer for use at low temperatures based on a high- Q silicon torsional oscillator. The oscillator is fabricated using standard lithographic techniques from a single-crystal silicon wafer. The sample stage of the oscillator has an area of 0.57 cm^2 and is suitable for deposition of thin magnetic film samples. Oscillator motion is detected through a capacitance measurement. The small torsion constant of the oscillator combined with a Q value $> 10^6$ allow detection of magnetic moments as small as 10^{-13} A m^2 . Magnetometer sensitivity is measured using small superconducting open cylinders machined from aluminum. © 1998 American Institute of Physics. [S0034-6748(98)03710-1]

I. INTRODUCTION

Silicon cantilever oscillators have been used as sensitive magnetometers in several configurations. For example, they find applications for use as vibrating reed magnetometers, in magnetic force microscopes,¹ for magnetic force resonance microscopy,² and for torque magnetometry, either in a torque nulling apparatus,³ or as an torsional oscillator torque magnetometer.⁴ Single-stage paddle oscillators have been used as torque magnetometers in high fields.⁵⁻⁷ In this article, we describe a torsional oscillator magnetometer specifically for measurement of the remanent magnetization of thin films. By utilizing a high- Q design and a small torsion constant, high sensitivity can be maintained even with a sample stage area that is orders of magnitude greater than those of other designs.

II. APPARATUS

This magnetometer design relies on the fact that a material with a magnetic moment \mathbf{m} in an external magnetic field \mathbf{B}_0 experiences a torque given by

$$\boldsymbol{\tau} = \mathbf{m} \times \mathbf{B}_0. \quad (1)$$

We can drive a macroscopic (yet highly sensitive) torsional oscillator by placing a sample of interest on it and applying a magnetic field at an angle with respect to the sample magnetization. A magnetometer can thus take advantage of the inherently low dissipation of the silicon oscillator,⁸ through the application of an ac drive magnetic field (\mathbf{B}_{dr}) at the resonant frequency of the torsional oscillator. The motion of the oscillator is then detected by measuring the voltage on a charged electrode brought up to a grounded portion of the oscillator.

The magnetometer consists of a two-stage torsional oscillator clamped in place near position detection electrodes and a coil which is used to generate a drive field. Because this is a macroscopic oscillator, it is relatively easy to deposit thin films on its surface. The oscillator support structure is designed to minimize vibrational coupling, and the coil support structure is designed to provide as much thermal and

vibrational isolation as possible between the coil and the oscillator. We will describe the oscillator performance together with results of a calibration using superconducting cylinders attached to the oscillator in a later section.

A. Silicon oscillator

At the heart of this design is a two-stage silicon oscillator fabricated from a single-crystal silicon wafer.⁹ Details of oscillator fabrication have been described elsewhere.¹⁰ Fabrication is based on a KOH anisotropic etch through a p -type $\langle 100 \rangle$ -oriented silicon wafer using a lithographically patterned Si_3N_4 layer as a mask. After the etch, the Si_3N_4 may be removed from one side of the oscillator, and the etch repeated to create thinner oscillators with smaller spring constants.

Our oscillator is illustrated in Fig. 1. The upper stage consists of a mass (the head) and a torsion rod (the neck) connected to the lower stage, with another mass (the wings) and torsion rod (the leg), connected to a base, which is used to mount the oscillator. We operated the oscillator in its antisymmetric mode, where head and wing motions are 180° out of phase. In vacuum at low temperatures, such oscillators can have Q values $\gg 10^6$. Oscillators with thicknesses of 150, 220, and $360 \mu\text{m}$ have been studied.

For a torsional oscillator driven at resonance, the amplitude of deflection, θ_0 is given by

$$\theta_0 = Q \frac{\tau_0}{\kappa}, \quad (2)$$

where Q is the oscillator Q factor, equal to 2π times the fractional energy lost per cycle, τ_0 is the amplitude of the sinusoidal drive torque, and κ is the torsional spring constant of the oscillator. This equation relates the parameters which can be adjusted to maximize torque sensitivity. In the antisymmetric mode, most of the oscillator motion occurs in the head, which has a much smaller moment of inertia compared to the wings, and so the total torsional spring constant of the system can be approximated by that of the neck.

The torsional spring constant can be calculated from the torsion rod geometry by assuming an approximately rectan-

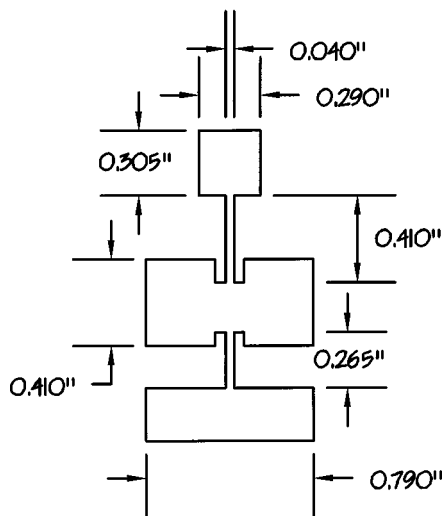


FIG. 1. Diagram of the geometry of the two-stage torsional oscillator. The oscillator is oriented so the head is at the top, the wings in the middle, and the base at the bottom.

gular cross section. A torsion rod of length l , and rectangular cross section of height a and width b has a torsional spring constant given by¹¹

$$\kappa = \beta \frac{ab^3}{l} G, \quad (3)$$

where β is a slowly varying function of the ratio a/b , $a > b$, and G is the shear modulus.

To allow sensitive detection of deflection, we measured oscillator motion by positioning electrodes a distance, s , from the wings to form a capacitor. The fixed electrodes are biased at a voltage, V , to enhance sensitivity [Eq. (4) below]. Motion is then measured by observing the change in voltage at these detection electrodes. Assuming this voltage variation is detected with a preamplifier coupled to the electrode through a cable with capacitance to ground C_e , and assuming the change in spacing δs is small with respect to s , the measured change in voltage, δV , is given by¹²

$$\frac{\delta V}{V} = \frac{\delta s}{s} \frac{C_e}{C_c + C_e}, \quad (4)$$

where C_e is the capacitance of the electrode capacitor. With the geometry we have employed and a voltage bias of 100 V, we achieve a sensitivity to wing displacement of better than 1 Å. However, because the oscillator must be run at its anti-symmetric resonant frequency to obtain a high- Q factor, the amplitude of oscillation of the oscillator wings is only 1/25th of the amplitude of the oscillator head. Nevertheless, there are several advantages to detecting oscillation at the oscillator wings. The wings provide a larger area for the capacitor, C_e , and are farther from the torsion axis so the change in capacitor separation, δs , will be greater for a given angular deflection. There is also no need for a conductive path to the head (which would increase dissipation at the neck of the oscillator) and the electrodes do not interfere with the magnetic drive at the sample.

Metal is deposited on wings, leg, and base of the oscillator through a machined aluminum mask. This provides

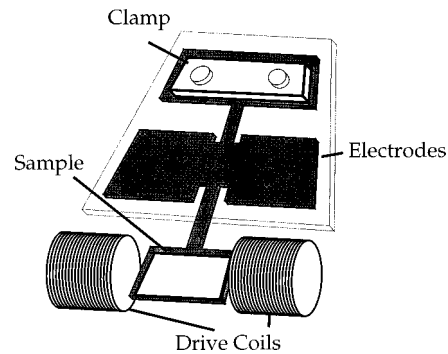


FIG. 2. Illustration of mounted oscillator showing geometry of drive coils and drive and detect electrodes.

matching electrodes for the biased detection electrodes to form detection capacitors, as well as a conduction path to ground through the clamp on the base.

The sample is attached to or evaporated onto the head of the oscillator. This is where an applied torque will most effectively drive the oscillator. It is possible to pattern a film deposited on the oscillator head using a liftoff technique, if the oscillator is attached to a backing wafer with some resist before resist is spun on and lithography is performed. If done properly, the oscillator will be freed from the backing wafer when the lift off occurs. We had some success using Shipley 1400-27 resist, which was allowed to set over night. Our yield was somewhat less than 50%, as some oscillators would slip off during spinning, or would not be properly released during liftoff.

The oscillator is clamped onto a mounting plate which contains integrated electrodes. This allows consistent separation between the electrodes that constitute the detection capacitor, and more reproducible sensitivity. This separation, s , is nominally 75 μm . The oscillator clamping plate is removable from the cryostat to allow easy mounting. After the oscillator is attached to the mounting plate, the mounting plate is bolted onto a vibration isolation stage, which is connected to the cryostat sample stage by a 1 in. long, 1/8 in. diameter copper rod. The sample stage is attached to the mixing chamber stage of a dilution refrigerator.

B. Drive coil

The drive is provided by two coils, each 450 turns of 0.005 in. multifilament NbTi superconductor clad with CuNi wound on a form with a diameter of 0.350 in., separated by 0.475 in. The coils are cast in epoxy with a gap machined between them where the oscillator head and the sample is to sit. (See Fig. 2.) These coils can generate ac magnetic fields of up to 1 mT in the kilohertz frequency range. The drive coil is mounted on a ring cast from Stycast 1266 epoxy, one third of which had been removed in order to allow it to fit around the oscillator. Three stainless-steel tubes were bonded into the epoxy. These run through holes in the sample stage of the cryostat so the drive coil can be raised out of the way to ease oscillator mounting. Set screws in the sample stage fix each tube in place during cool down and measurement. The drive coil and drive coil leads are heat sunk to the 1 K pot.

TABLE I. Calculated properties of several oscillators. 1 and 2 correspond to the two calibration oscillators. 3 is an uncalibrated oscillator.

Oscillator	1	2	3
Thickness (μm)	360	220	150
κ_{neck} (Nm)	4.3×10^{-2}	1.1×10^{-2}	3.8×10^{-3}
Frequency (Hz)	2378	1590	1120
(antisymmetric mode)			
Measured Q	3×10^6	3×10^6	$\sim 10^5$
Minimum drive torque (Nm)	8×10^{-14}	2×10^{-15}	$\sim 2 \times 10^{-14}$
Sensitivity w/ 100 V bias ($V_{\text{out}}/V_{\text{in}}$ per emu)	4.4×10^2	4.1×10^3	$\sim 4 \times 10^2$
Measured sensitivity ($V_{\text{out}}/V_{\text{in}}$ per emu)	2.1×10^2	2.2×10^3	
Minimum magnetization to drive (A m^2)	4.6×10^{-12}	4.7×10^{-13}	$\sim 5 \times 10^{-12}$

III. PERFORMANCE

The torsional spring constant of our oscillators varied from 3.8×10^{-3} Nm for our thinnest oscillator to 4.3×10^{-2} Nm for our thickest. (See Table I.) We have found that the Q factor of the oscillators can be increased by removing the glassy Si_3N_4 layer. Oscillators with Si_3N_4 on both faces generally have a Q factor of 6×10^6 , while oscillators with Si_3N_4 layers partially removed with HF show Q factors of 1.1×10^7 .

Our sensitivity to oscillator displacement is theoretically limited by thermal noise in the oscillator or noise in the oscillator detection circuitry. The rms noise for our thinnest oscillator at resonance should be $\langle \delta\theta^2 \rangle^{1/2} \sim \sqrt{4k_B T Q \Delta f / \kappa \omega_0}$.⁴ At 10 K, with a bandpass filter of bandwidth 10 Hz, this yields an amplitude of 3×10^{-8} rad on our smallest oscillator. When the ratio of paddle to head angular displacement (1:25), and the average distance of the paddle electrode from the torsion axis (~ 0.5 cm) are taken into account, we arrive at a resolution of paddle displacement of ~ 0.04 Å. Thermal noise may contribute significantly to signal degradation. Other possible sources of noise are electrical noise in the coaxial cables, and thermal noise in voltage bias capacitors and resistors. The Johnson noise due to the resistor in the bias box connected with the circuit is given by $\langle \delta V^2 \rangle^{1/2} = \sqrt{4k_B T R \Delta f} \approx 6 \times 10^{-7}$ V, assuming a bandwidth of 10 Hz. This corresponds to an uncertainty of about 4×10^{-3} Å in oscillator position. In practice the lock-in amplifier, a PAR124A, which maintains a phase-lock loop (shown in Fig. 3), loses phase-lock when the amplitude of the oscillator paddles drops below 0.4 Å. This may be due to acoustic vibrations in the coaxial leads that create spurious voltage oscillations which draw the PAR124A away from resonance. 0.4 Å of paddle motion corresponds to 3×10^{-7} rad angular deflection in the oscillator head. This provides a lower limit on detectable signal, though our resolution of this signal is better than 10%, so our sensitivity to magnetization will be an order of magnitude better. If all oscillators had a Q value of 1×10^7 , the minimum torque drive to run these oscillators would vary from 1.1×10^{-17} to 1.3×10^{-16} Nm. Given the limit on our drive field of 1 mT, this would require a minimum magnetization of approxi-

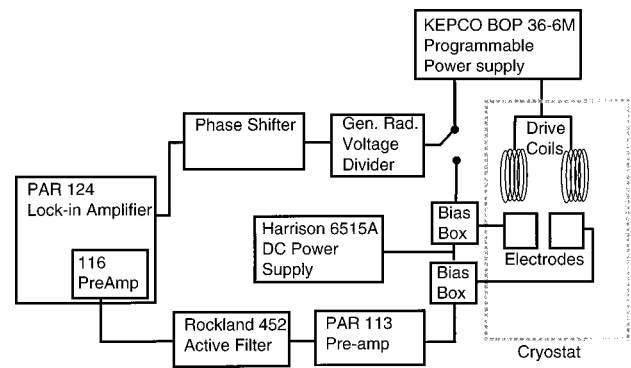


FIG. 3. Block diagram of oscillator drive and detection circuit. The signal monitor on the PAR 124 lock-in amplifier is connected to its external reference input, thus causing it to output an ac drive voltage at the frequency of the detected signal.

mately 10^{-14} A m^2 to allow the thinnest oscillator to be driven.

In Table I we present data on several oscillators that we have characterized. We measured the Q factor and frequency for each oscillator. In each case, the Q factor is less than what has been found in the majority of the oscillators we have studied. For oscillators 1 and 2, this is due to the fact that a superconducting sample has been attached to the head of the oscillator with a little epoxy, which increases dissipation. For oscillator 3, it is not clear why the Q has been so adversely affected. It is possible that a crack formed in the silicon during the thinning process which then served as a source of dissipation.

It is possible to calculate the sensitivity of the oscillator from the mechanical properties. The most useful units of sensitivity when doing an experiment is the ratio of the amplitude of voltage change at the detection preamplifier, V_{out} , to amplitude of voltage applied to the drive coil, V_{in} , per emu of magnetic moment. The calculated values of sensitivity in these units is also shown in Table I. Note that this measurement of sensitivity increases more rapidly than Q/κ because the current into the drive coil for a given voltage increases inversely as the resonant frequency.

In order to compare the sensitivity of the oscillator with its predicted value, we attached a cylindrical ring of aluminum to the heads of oscillators 1 and 2 (Fig. 4). Given this

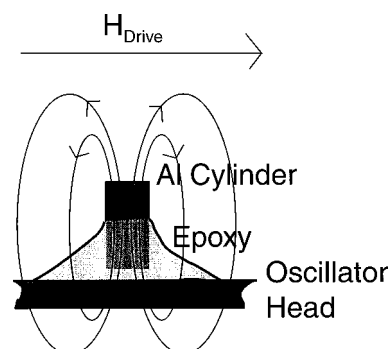


FIG. 4. Schematic of calibration using an Al cylinder. The cylinder is attached to the oscillator with epoxy. When it is cooled through the superconducting transition, it traps magnetic flux, and so has a calculable magnetic moment.

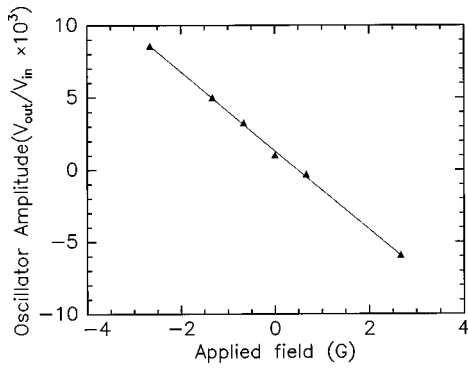


FIG. 5. Measured magnetometer response vs magnetic field for first Al cylinder measured. These measurements were taken after the applied field had been removed, and so the only contribution to the torque is due to the magnetization of the cylinder. The oscillator used for this measurement was not thinned. The slope of this linear fit (solid line) provides us with a measurement of the magnetometer sensitivity.

geometry, we expect that the cylinder will trap an amount of flux approximately equal to an applied external field multiplied by the area of the cylinder bore when it is cooled through its superconducting transition temperature, T_c , in that field. We can estimate the supercurrent necessary to generate this flux, and from this, estimate the magnetic moment of the cylinder. This will provide a calculable amount of torque exerted by the applied driving field. We will also look for torque due to the demagnetization factor.

We show magnetization data for two such cylinders in Figs. 5 and 6. Both cylinders had an i.d. of $460 \mu\text{m}$ and an o.d. of $560 \mu\text{m}$. The first was 1 mm long and the second 1.5 mm long. We have plotted voltage output (V_{out}), divided by the drive (V_{in}) as a function of cooling field for each oscillator. V_{out} is the amplitude of the voltage detected at the capacitive pickup, and V_{in} is the amplitude of the voltage applied to the magnetic coil in series with a 2.5Ω resistor. Empirically, the smallest voltage we can lock onto with the PAR 124A is about $3.5 \mu\text{V}$. The largest drive voltage we can apply before the coil is driven normal is about 1.5 V. This implies that the smallest value of $V_{\text{out}}/V_{\text{in}}$ is about 2×10^{-6} .

We can use the simple model that each cylinder is a solenoid that generates an internal field equal to the applied

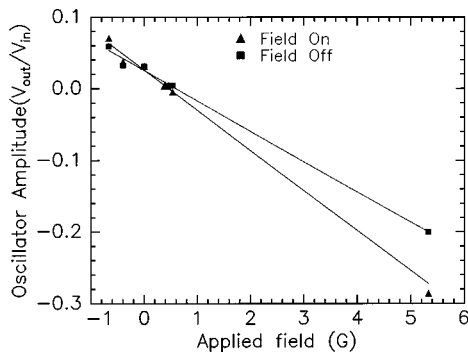


FIG. 6. Measured magnetometer response vs magnetic field for second Al cylinder measured. Measurements were taken both with no applied field (squares) and with an applied field (triangles). In the latter case, there was an additional torque due to demagnetization effects. The oscillator used for this measurement was thinned.

field. In this case, the magnetic moment of the cylinder will be equal to the volume of the cylinder v times the magnetizing field, B_0 , divided by μ_0 . The magnitude of the torque exerted by a driving field, B_{dr} , is then

$$\tau_0 = \frac{v B_{\text{dr}} B_0}{\mu_0} \tag{5}$$

In the case of the first cylinder, the volume is $1.64 \times 10^{-10} \text{ m}^3$, so the magnetization is $1.3 \times 10^{-8} \text{ A m}^2/\text{G}$. We find $|V_{\text{out}}/V_{\text{in}}| = 2.7 \times 10^{-3}/\text{G}$ (or equivalently, 210/emu). This implies that the minimum magnetization at which the first oscillator can operate is $1 \times 10^{-11} \text{ A m}^2 (1 \times 10^{-8} \text{ emu})$. Of course, the sensitivity is at least a factor of 10 better than this; this is only the minimum magnetization for which we can sustain a phase-locked loop.

The second oscillator was fabricated to study the effect of chemically thinning on oscillator sensitivity. The nitride layer was removed on its rough side, and an additional KOH etch was performed. The etch reduced the resonant frequency of the oscillator from 2378 to 1590 Hz. Q^{-1} was still 3×10^{-7} so the decreased torsion constant greatly increases sensitivity. For this oscillator, we see a response in $|V_{\text{out}}/V_{\text{in}}|$ of 0.042/G (equivalently, 2200/emu). Taking into account that the volume of this cylinder is 50% greater, we calculate a minimum magnetization of $1 \times 10^{-12} \text{ A m}^2$. (See Table I.)

We measured the magnetic torque both with and without the magnetizing field (B_0) left on. With the field, there is increased torque. We can calculate the expected demagnetization torque using the sample averaged demagnetization factor from Brown.¹³ He found that for a cylinder with a length to diameter ratio of 1.5, $N_{\text{m}\parallel}$ —the magnetometric demagnetization factor along the cylinder axis—is approximately 0.25. $N_{\text{m}\perp}$ is then 0.375. The difference between these, ΔN approximately equals 1/8. Using the fact that $\chi_{\text{sc}} = -1$, we can solve for the average superconductor magnetization, \mathbf{I} , in an applied field $\mathbf{H}_0 (= \mathbf{B}_0/\mu_0)$ using the equation¹⁴

$$\langle \mathbf{I} \rangle = \mu_0 \chi (\mathbf{H}_0 + \mathbf{H}_D) = \mu_0 \chi \mathbf{H}_0 - \chi N_{\text{m}\parallel} \mathbf{I}, \tag{6}$$

where \mathbf{H}_D is the demagnetizing field, to find that along the axis of the cylinder

$$\langle I \rangle \approx -\frac{4}{3} \mu_0 H_0. \tag{7}$$

We can insert this into the expression for demagnetization torque,

$$\tau = \frac{H_0 \Delta N I^2 / \mu_0}{H_0 + \Delta N I / \mu_0} \theta, \tag{8}$$

along with the demagnetization factor difference of 0.125, to obtain

$$\tau \approx \frac{1}{8} \frac{(4/3)^2 \mu_0 H_0^2}{[1 - (4/3)(1/8)]} v \theta, \tag{9}$$

where v is the sample volume. We are only interested in the time dependent part of θ , which can be approximated for small drive fields (B_{dr}) by

$$\theta \approx \frac{B_{\text{dr}}}{B_0}. \quad (10)$$

Substituting B_0/μ_0 for H_0 , we are left with an expression for the amplitude of the time varying demagnetization torque

$$\tau_0 = \frac{4vB_{\text{dr}}B_0}{15\mu_0}, \quad (11)$$

which is 4/15 the torque due to the magnetization. [See Eq. (5).] This will be quite sensitive to the actual geometry, which may account for the actual relative increase in torque being about 1/3, greater than that predicted.

The measured sensitivities are reduced by approximately 1/2 with respect to the calculated values. This is possibly because the separation between detection electrode and paddle may be greater than it was designed to be, as the paddle may “flop” a little under the influence of gravity.

ACKNOWLEDGMENTS

The authors would like to thank the Cornell Node of the National Nanofabrication Network, where oscillator fabrica-

tion was carried out. Support was provided by the Cornell Material Science Center under DMR-9632275.

¹Y. Martin and H. K. Wickramasinghe, *Appl. Phys. Lett.* **50**, 1455 (1987).

²J. A. Sidles *et al.*, *Rev. Mod. Phys.* **67**, 249 (1995).

³M. Chaparala, O. H. Chung, and M. J. Naughton, *AIP Conf. Proc.* **273**, 407 (1993).

⁴C. Rossel *et al.*, *J. Appl. Phys.* **79**, 8166 (1996).

⁵P. L. Gammel, L. F. Schneemeyer, J. V. Wasczak, and D. J. Bishop, *Phys. Rev. Lett.* **61**, 1666 (1998).

⁶R. N. Kleiman, P. L. Gammel, E. Bücher, and D. J. Bishop, *Phys. Rev. Lett.* **62**, 328 (1989).

⁷P. A. Crowell *et al.*, *Rev. Sci. Instrum.* **67**, 4161 (1996).

⁸R. E. Mihailovich and J. M. Parpia, *Phys. Rev. Lett.* **68**, 3052 (1992).

⁹R. N. Kleiman *et al.*, *Rev. Sci. Instrum.* **56**, 2088 (1985).

¹⁰G. Kaminsky, *J. Vac. Sci. Technol. B* **3**, 1015 (1985).

¹¹H. Ford, *Advanced Mechanics of Materials* (Longmans, Green and Co. Ltd., London, 1963).

¹²G. K.-S. Wong, in *Experimental Techniques in Condensed Matter Physics at Low Temperatures*, edited by R. C. Richardson and E. N. Smith (Addison-Wesley, Redwood City, CA, 1988), Chap. 4.2.

¹³W. F. Brown, *Am. J. Phys.* **28**, 542 (1960), as cited in Zijlstra, 1967.

¹⁴H. Zijlstra, *Experimental Methods in Magnetism* (Wiley, New York, 1967).